JOC The Journal of Organic Chemistry

Article

pubs.acs.org/joc

Mechanistic Studies of Bismuth(V)-Mediated Thioglycoside Activation Reveal Differential Reactivity of Anomers

Manibarsha Goswami,[†] Daniel C. Ashley,[‡] Mu-Hyun Baik,*[,‡,§,∥] and Nicola L. B. Pohl*[,‡,⊥]

[†]Department of Chemistry, Iowa State University, Ames, Iowa 50011, United States

[‡]Department of Chemistry, Indiana University, Bloomington, Indiana 47405, United States

[§]Center for Catalytic Hydrocarbon Functionalizations, Institute for Basic Science (IBS), Daejeon 305-701, Korea

[∥]Department of Chemistry, Korea Advanced Institute of Science and Technology (KAIST), Daejeon 305-701, Korea

[⊥]Department of Chemical and Biological Engineering, Iowa State University, Ames, Iowa 50011, United States

Supporting Information

ABSTRACT: The mechanism of bismuth(V)-mediated thioglycoside activation was examined using reaction kinetics and quantum chemical reaction models. NMR experiments show an unusual nonlinear growth/decay curve for the glycosylation reaction. Further studies suggest an anomeric inversion of the β-glycoside donor to the α-donor during its activation, even in the presence of a neighboring 2-position acetate. Interestingly, in situ anomerization was not observed in the activation of an α-glycoside donor, and this anomer also showed faster reaction times and higher product diastereoselectivites. Density functional theory calculations identify the structure of the promoter triphenyl bismuth ditriflate, $[Ph_3Bi(OTf)_2$, **1**$]$, in solution and map out the energetics of its interactions with the two thioglycoside anomers. These calculations suggest that **1** must bind the thiopropyl arm to induce triflate loss. The computational analyses also show that, unlike most *O*-glycosides, the β- and α-donor *S*-glycosides are similar in energy. One energetically reasonable anomerization pathway of the donors is an S_N1-like mechanism promoted by forming a bismuth-sulfonium adduct with the Lewis acidic Bi(V) for the formation of an oxacarbenium intermediate. Finally, the computed energy compensations needed to form these α vs β Bi adducts is a possible explanation for the differential reactivity of these donors.

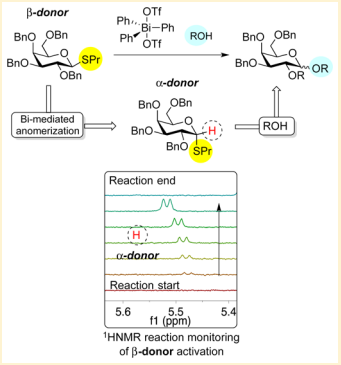

INTRODUCTION

Carbohydrates are vital to life; they form the building blocks of lipopolysaccharides, glycoproteins, and glycolipids[1−3] and constitute key components of natural products and pharmaceuticals,[4,5] such as the antimicrobials vancomycin[6] and the cardiac glycosides.[7] Thus, the ability to manipulate the chemical composition of carbohydrates in a controlled and scalable fashion is paramount to increased understanding of their roles.[1] Despite significant efforts to predict the outcome of the glycosylation reactions that are key to linking monosaccharides into more complex structures, the dearth of mechanistic studies has prevented the development of reliable rules.[8,9] Although an exciting number of strategies have been developed, neighboring group participation (NGP) from the 2-position remains one of the most reliable methods for setting the anomeric stereocenter.[10,11,8,12,13] Nonetheless, reactant concentrations, the nature of the leaving group and its mode of activation, substituents and their effects on carbohydrate conformations, steric hindrance, metal coordination, temperature, and solvent effects have also been noted as factors that affect reaction stereoselectivity.[5] Clearly, nucleophilic substitution of some type at the anomeric C-1 carbon is at play (Scheme 1) with some degree of oxacarbenium ion formation,[14,15] which is perceived to form by the dissociation of activated glycosyl donor−promoter complexes.[16,17] Nuclear magnetic resonance (NMR)-based mechanistic studies of chemical glycosylations carried out in the past two decades have been reviewed recently.[18] However, very few glycosylation reactions have been subjected to comprehensive mechanistic studies—detailed experimental and analytical investigations along with in-depth computational analyses.[16,19,20]

Recently, we developed a novel method for activating thiopropylglycosyl donors (**2**) and coupling them to various acceptors that employed triphenylbismuth ditriflate (**1**) as the promoter (Scheme 2).[21] Bismuth is attractive for its high abundance and relative lack of toxicity; however, little is known about its reactivity patterns, especially starting with Bi(V) species.[22−25] The high valent bismuth center could act as a soft Lewis acid that interacts with the Lewis basic site of the thioglycoside. Bismuth can also easily access the common oxidation states of (III),[26,27] (IV), and (V), which offers an opportunity to access redox-enhanced reaction mechanisms. Excellent yields were obtained in this particular Bi(V)-mediated glycosylation reaction without using additional copromoters or additives, and the strategy was extended to a wide range of carbohydrates with remarkable functional group tolerance, including of alkenes and alkynes.[28] Surprisingly, we observed that a promoter containing Bi(V) could activate the thioglycosyl donors, whereas the more common

Received: April 16, 2016
Published: June 13, 2016

DOI: 10.1021/acs.joc.6b00860
J. Org. Chem. 2016, 81, 5949−5962

Scheme 1. Chemical Glycosylation Pathways Leading to 1,2 *trans*- and 1,2 *cis*-Glycosides

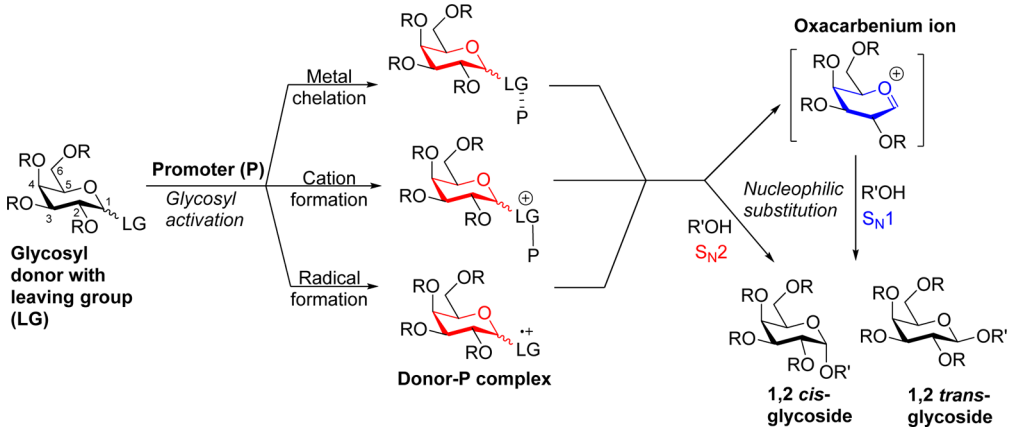

Scheme 2. General Scheme for Thiopropylglycoside Activation with Pentavalent Bismuth 1

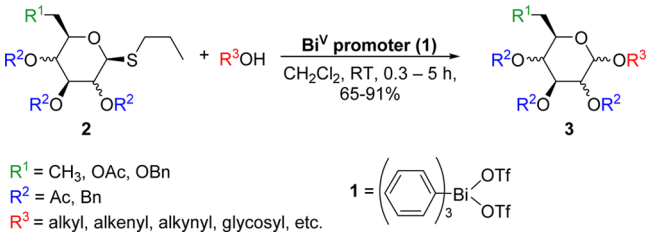

Bi(III) analogues or triflic acid alone could not. In addition to being sufficiently reactive even when substoichiometric amounts of the promoter [$Ph_3Bi(OTf)_2$] were added, these reactions could also be performed at room temperature, which are distinctively different, attractive features that are not commonly observed in previous methods for thioglycoside activation.[21]

This newly discovered reactivity pattern for Bi(V), however, leaves many questions as to how the reaction works, especially given the paucity of mechanistic studies of bismuth-mediated reactions. Even the thioglycoside, one of the most commonly used building blocks in carbohydrate synthesis, has only spawned mechanistic work focused primarily on the initial activation step with the reactive sulfonium intermediate having received special attention.[29−31] Several key mechanistic questions remain unanswered to date: What are the exact structures of the reactive intermediates? What are their conformational preferences and which chemical features might govern the stereospecificity of the reaction?

RESULTS AND DISCUSSION

One of the most fundamental tasks for deciphering a reaction mechanism is determining the rate law, which requires careful and a sometimes challenging series of studies. Precise chemical kinetics studies on glycosylation are rare; Vernon et al.[32−35] and Schroeder et al.[36] were among the first who attempted to study the kinetics of a Koenigs−Knorr-type glycosylation by combining polarimetry and gas liquid chromatography (GLC) techniques. Following Wong and co-workers' relative reactivity work in thioglycoside building blocks,[37] Huang and co-workers determined relative rates of reactions of thioarylglycosides, which were activated by a mixture of *N*-iodosuccinimide (NIS) and trifluoromethanesulfonic acid (TfOH).[38] Special attention was given to various substituent effects in this study. To investigate the kinetics of activation and to identify the rate-determining step of the bismuth-mediated reaction, we carried out a series of variable-temperature NMR studies, which can be challenging due to signals that originate from different glycosyl reactants/products in solution that may overlap with the characteristic signals that must be monitored.[18] A benzylated β-thiopropyl galactoside was selected to be the glycosyl donor (**4-*β***), and methanol (CH_3OH, **5**) was chosen as the glycosyl acceptor for its simplicity (**5**) along with the bismuth complex $Ph_3Bi(OTf)_2$ (**1**) as the promoter (Figure 1a). Although prior exploratory experiments

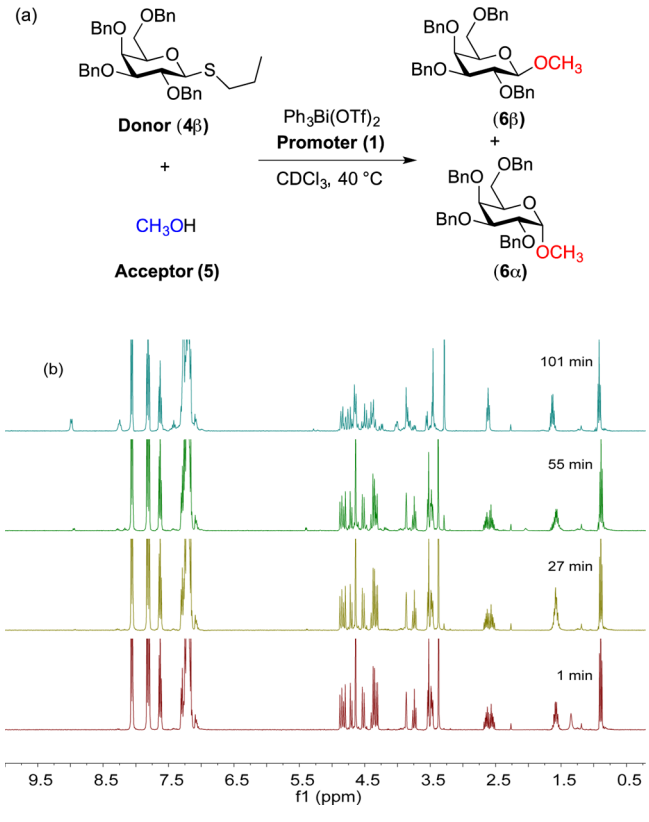

Figure 1. (a) Model glycosylation with β-donor for rate-order studies; (b) reaction progress monitored by ^{1}H NMR spectra of model glycosylation reaction.

were carried out in dichloromethane (CH_2Cl_2), these experiments were conducted in chloroform-D ($CDCl_3$, 1H δ = 7.26 ppm) instead of CD_2Cl_2 (^{1}H δ = 5.32 ppm). This solvent was chosen to avoid overlapping (^{1}H)-peaks with the sugar-ring protons, thiopropyl, or the Bi(V) compound. After some experimentation,

DOI: 10.1021/acs.joc.6b00860
J. Org. Chem. 2016, 81, 5949−5962

we found that 313.15 K (40 °C) was the optimum temperature for monitoring reaction kinetics, considering the required reaction time of a single experiment on the NMR instrument. Figure 1b shows the ^{1}H NMR data collected for this glycosylation reaction.

The progress of the reaction was monitored by measuring the disappearance and appearance of the methoxy peak in the reactant (**5**, δ = 3.47 ppm) and β-product (**6-β**, δ = 3.38 ppm), respectively, as illustrated in Figure 2a. These peaks were selected

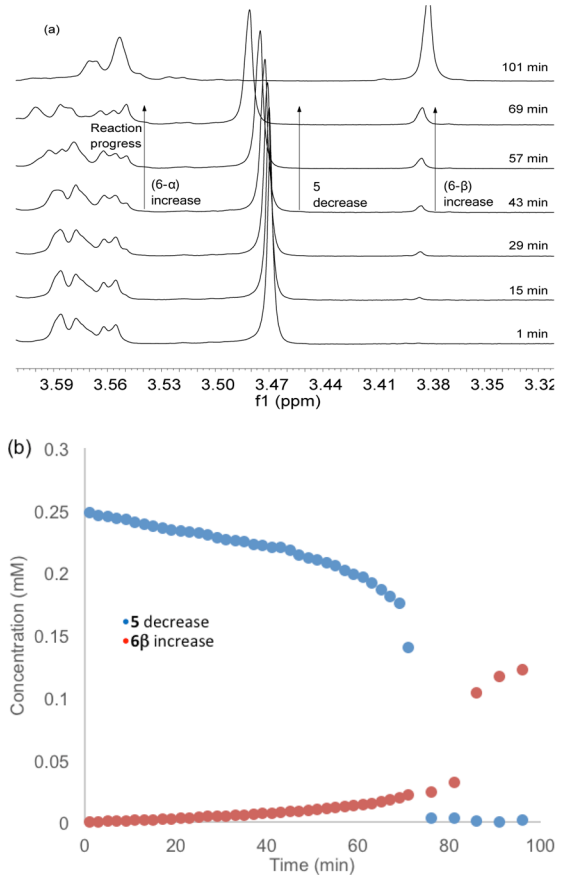

Figure 2. (a) Expanded ^{1}H NMR spectrum of model glycosylation showing the peaks of interest; (b) product and acceptor concentration vs time. Reaction conditions: **4-β**:**1**:**5**::1:1:1 equiv, 40 °C, $CDCl_3$.

as they do not overlap with the other proton peaks of interest and could thereby be accurately integrated. The relative concentrations of these species derived from the numerical integration of the NMR signals against reaction time is shown in Figure 2b. A gradual decrease of the OCH_3 signal, highlighted in blue in Figure 2b, indicates the depletion of **5** and correlates with an increase of the OCH_3 signal of **6-β**, shown in red. Interestingly, the concentration traces show a relatively long incubation time characterized by a slow and steady decay of **5** accompanied by an even slower but equally steady increase of **6-β**. At ∼70 min, there was a sudden drop in the concentration of **5** paired with a similarly sharp increase in the **6-β** concentration.

This nonlinear behavior in the consumption of **5** and production of **6-β** is unusual and not commonly observed in standard organic reactions.[39−41] Plausible speculation is that the initial, slow induction phase is related to transforming the Bi(V) promoter to its active form. Once the promoter has passed through the resting state, a rate escalation is observed, and the glycosylation reaction proceeds to completion. One obvious scenario is that the promoter activation step is unimolecular, i.e., does not involve **5**. If so, simply incubating the promoter in the reaction solution that lacks **5** for ∼80 min and adding reactant **5** to the solution should show an immediate reaction. Our experiments show, however, that this is not the case, thereby indicating that nucleophile **5** is required for the activation of the promoter and suggesting that its activation is not unimolecular. These interesting features require deeper investigation into the influence of the substrates or reactants on the reaction kinetics.

The time-resolved ^{1}H NMR spectra (Figure 1b) reveal interesting additional features. Magnification of the relevant chemical shift ranges is shown in Figure 3. In the range of 5.5−5.6 ppm (d, J = 4.8−5.2 Hz, 1H), there is a doublet signal that grew in strength during the course of the reaction and disappeared as soon as all of the reactant was consumed. Similarly, multiplets at 2.7 and 1.6 ppm appear to split into two sets as the reaction proceeded, and this trend also disappeared at the end of the reaction. These observations are consistent with the formation of a reactive intermediate, that is ultimately consumed when the reaction goes to completion. This discovery is exciting; the direct detection of reactive intermediates in glycosylation reactions is rare,[18,29,31,42,43] and particularly so in this case, given that these experiments are not low-temperature studies and involve a metal, bismuth, as a promoter. As illustrated in Scheme 1, these intermediates can form by a variety of pathways when the promoter acts on a glycosyl donor.

In our case, the growing doublet peak around 5.5 ppm can be assigned to the β-anomeric H-1 that is usually found in the range of 4.5−6.5 ppm. Interestingly, this doublet peak shifted approximately 0.02 ppm during the course of the reaction, as illustrated in Figure 3. Moreover, the peak initially seemed to have a coupling constant of 4.8 Hz, which later increased slightly to 5.5 Hz. This spectral signature is intriguing and suggests the existence of a dynamic equilibrium between two closely related glycosyl species during the activation. If formation of a β-glycosyl sulfonium intermediate[30,31,42,43] is considered from the β-donor, then the anomeric H-1 proton peak is expected to be more deshielded than what a chemical shift of 5.5 ppm indicates, and the coupling constant should be in the range of 9−11 Hz.

Next, we looked into the possibility of the formation of a thiogalactoside radical cation. Previously, thioglycosides have been activated by a single-electron transfer (SET) mechanism by methods such as anodic oxidation or UV- or visible-light activation in the presence of photosensitizers.[44,45] For probing the possibility of this SET pathway, glycosylations were carried out (benchtop and NMR-based) in the presence of radical scavengers (Galvinoxyl, TEMPO), which can trap radical intermediates and terminate radical-mediated activation. Interestingly, the addition of these scavengers to the reaction mixture has no effect on the activation and still leads to the formation of the desired products (see Supporting Information for details). Therefore, we concluded that the Bi promoted activation does not follow a radical pathway or form any in situ radical thioglycoside intermediates.

Another plausible intermediate that can be envisioned in the course of triaryl Bi(V)-mediated reactions is phenylation of the substrates, typically containing alcohols, amines, or thiols.[24] If the thiopropylglycoside is phenylated to form a reactive species, we expected to observe phenylpropyl sulfide (PhSPr) as one of the byproducts during the activation. To analyze the presence of PhSPr, we conducted gas chromatography−mass spectrometry (GC-MS)-based studies. The model glycosylation (Figure 1a, room temperature instead of 40 °C) was monitored at different time

DOI: 10.1021/acs.joc.6b00860
J. Org. Chem. 2016, 81, 5949−5962

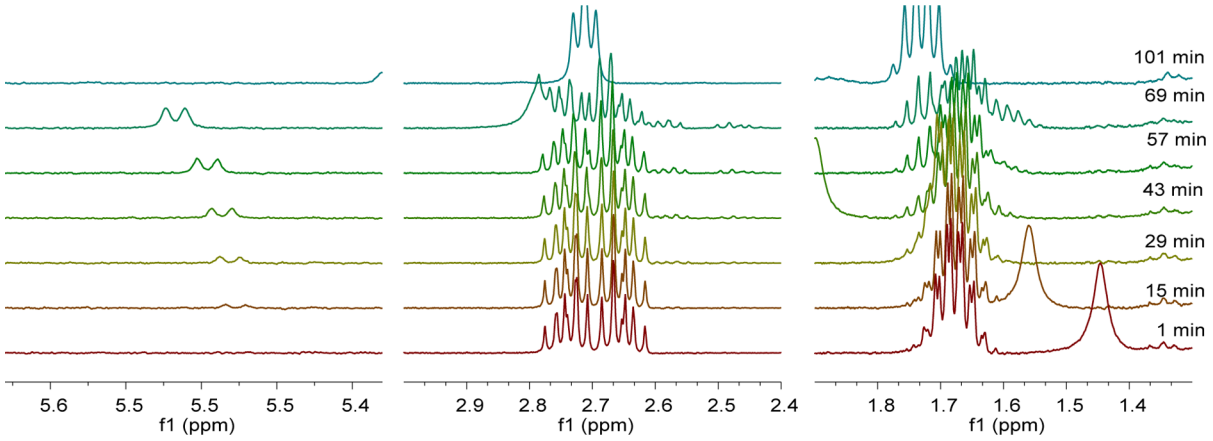

Figure 3. Expanded regions of the kinetics NMR spectra focusing on the transient peaks.

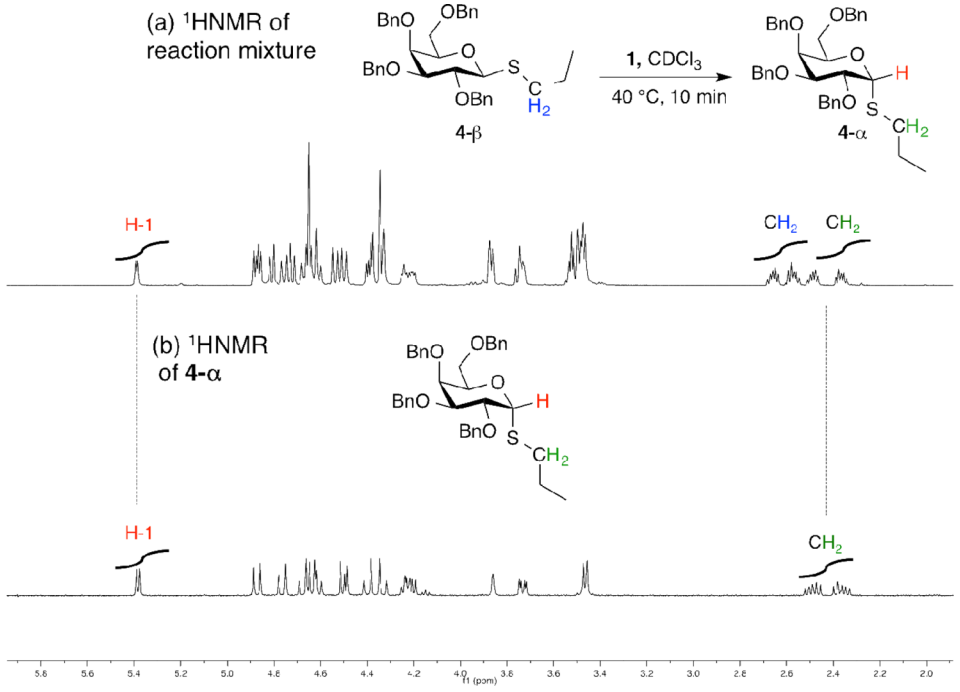

Figure 4. ^{1}H NMR comparison of the reaction mixture and **4-*α*** donor.

intervals [time (t) = 0, 25, 60 min (reaction end)]. We did not observe PhSPr (even in trace amounts) at any of these time points of the thioglycoside activation, a fact that suggests that a phenyl transfer from the triaryl Bi(V) promoter to the donor probably does not take place. We then synthesized PhSPr,[46] added it to a model glycosylation (Figure 1a) that has gone to completion, and probed the mixture by NMR. The addition of PhSPr to the reaction did not increase the intensity of the existing peaks in the NMR spectrum but created new peaks in the phenyl and alkyl regions. This observation supports the GCMS results that PhSPr is not formed in the reaction and that phenylation of the thioglycoside does not occur during the glycosylation. Looking closely at the NMR peaks, we considered that the observed chemical shifts and coupling constants may originate from an α-anomeric H-1 proton of a glycosyl compound, suggesting that an anomerization reaction had taken place. For this idea to be tested, a number of 1D and 2D correlation NMR studies were conducted on this intermediate. To maximize the population of this intermediate in solution, we mixed the donor (**4-*β***) and promoter (**1**) in the absence of an acceptor (**5**) under the same conditions as employed before. As soon as the intermediate signal was observed, 1D and 2D NMR spectra were obtained and compared to the benzylated α-thiopropyl galactoside donor. Correlating ^{1}H NMR (Figure 4) and ^{13}C as well as phase-edited HSQC spectra (see Supporting Information), we were able to establish that this intermediate was the α-donor, thereby confirming the hypothesis that the β-thioglycosyl donor anomerizes to the α-anomer during the reaction course. The discovery of this in situ anomerization then opened the question of which anomer was actually reacting in the bismuth-mediated glycosylation.

The anomeric effect—a preference of the axial versus equatorial glycosidic linkage—has been well-studied since its discovery in the 1950s. This effect is generally found to be larger for *O*-glycosides compared to that for *S*-glycosides owing to the lower electronegativity of sulfur compared to oxygen.[47] Nonetheless, few reports have demonstrated the utility of anomerization in thioglycosides to preferentially generate α-glycosides. Interestingly, Boons et al. in their report[48] mentioned that the thioglycosides with small thioalkyl groups could be anomerized via an intermolecular exchange in the presence of catalytic iodonium promoters.

DOI: 10.1021/acs.joc.6b00860
J. Org. Chem. 2016, 81, 5949−5962

In another case, Murphy and co-workers studied Ti- and Sn-catalyzed anomerization of uronic acids and acetylated thioglycosides and proposed a chelation-induced endocyclic ring cleavage mechanism for the anomerization.[49] However, in both of these cases, the anomerization was achieved under thermodynamic conditions[50] unlike our NMR and benchtop experiments, which are kinetically controlled. Therefore, a thermodynamic property like the anomeric effect[50] might not cause the $\beta \rightarrow \alpha$ anomerization of donors during the Bi(V)-mediated activation. Here, we want to highlight that, whereas the direct observation of carbohydrate anomerization is common, the possible role of such anomerization processes in ongoing glycosylation is largely ignored. Such an epimerization process has only been reported[51,52] by Poletti and co-workers; they found that β-trichloroacetimidate donors in ionic liquids—an uncommon glycosylation reaction medium—epimerize to the α-donor and also convert to the α-triflate intermediate during their activation by strong acids. Glycosylations are often conducted with the β-isomers of glycosyl donors such as thioglycosides; the 1,2 *trans*-isomers or C-1 β-donors for most sugars are easier to prepare utilizing the NGP of the C-2 oxygen protecting group, such as esters or phthalates. On the other hand, the 1,2 *cis*-isomers or the α-donors are more difficult to form in a stereoselective fashion and are often obtained by purification of an α:β product mixture derived from a reaction where the C-2 position is decorated with a nonparticipating group, such as benzyl ethers or silyl ethers, if they are not just used as a mixture of anomers in the glycosylation reaction.

To better understand this intriguing anomerization process and its role in the bismuth-mediated reaction mechanism, we considered whether the α-thioglycoside would exhibit the same kinetic behavior as the β-thioglycoside. For investigating this, the α-thioglycoside donor **4-α** was prepared and treated under the same glycosylation conditions as described for **4-β** (Figure 5a). Figure 5b compares the product fractions of the α-donor to those we had determined using the β-donor activation. The notably more rapid increase of the product fraction shown in red in Figure 5b indicates that the "more stable" α-donor reacts considerably faster than the β-donor (76 vs 101 min). The ^{1}H NMR spectra of kinetics data for **4-α** are presented in Figure 6a and show that the H-1 peak of **4-α** at δ 5.5 ppm displays several characteristic features during the activation (Figure 6b). First, the area under this doublet peak consistently decreased with reaction progress, which indicates that there was continuous consumption and either no or much slower formation of the **β** donor during the activation. This observation is consistent with the notion that the glycosylation is faster because **4-α** does not need to undergo the ($\beta \rightarrow \alpha$) anomerization that is required for **4-β.** Second, the coupling constant of this doublet or, in other words, the shape of the peak changed from a fine doublet (J = 5.4 Hz) to a broad singlet. This characteristic was also seen with the peak at 5.5 ppm toward the end of **4-β** donor activation. Interestingly, the peaks at δ 2.5 and 1.6 ppm corresponding to the methylene protons on the thiopropyl group (SCH_2CH_2-) also decayed with progress of the reaction. Unlike what is shown in Figure 3, the multiplicity of these two peaks do not seem to change, and a similar multiplet did not appear in the ^{1}H NMR spectrum. A sharp triplet (δ 2.7 ppm) and a quartet (δ 1.7 ppm) peak were found to grow as the reaction progressed.

These peaks may be assigned to methylene protons of the byproduct containing the thiopropyl moiety. Apart from the improved reaction time—an important discovery for the application of these glycosylation reactions to automated protocols—the diastereoselectivity of the obtained products is enhanced from 1:1 to a 1:1.8 ratio in favor of the β-anomer. This discovery leads to an improvement of our current methodology as the previous glycosylation trials did not produce high stereoselectivites in the products. Interestingly, we still observed the initial slow rise followed by the sudden rate escalation in the kinetic spectrum of the α-donor (Figure 5b) as seen with the β-donor. This finding suggests that the $\beta \rightarrow \alpha$ anomerization process is not responsible for the nonlinearity, and a promoter/catalyst activation step is involved during the activation.

To gain a deeper understanding of how bismuth promoter **1** interacts with the thioglycosides in solution and to construct a model that incorporates the experimental findings reported above, we carried out a series of quantum chemical calculations using density functional theory (DFT). Although theoretical studies of bismuth-containing systems are less common than studies on completely organic or transition metal-containing systems, a significant amount of work has shown that DFT can be effective for modeling Bi(III) chemistry,[53−61] although dispersion corrections are often needed. Fewer studies have been performed on Bi(V) systems; however, there are some notable examples.[62,63] Assuming that the Bi(V) species acts as a Lewis acid, one plausible mode of interaction may be its coordination

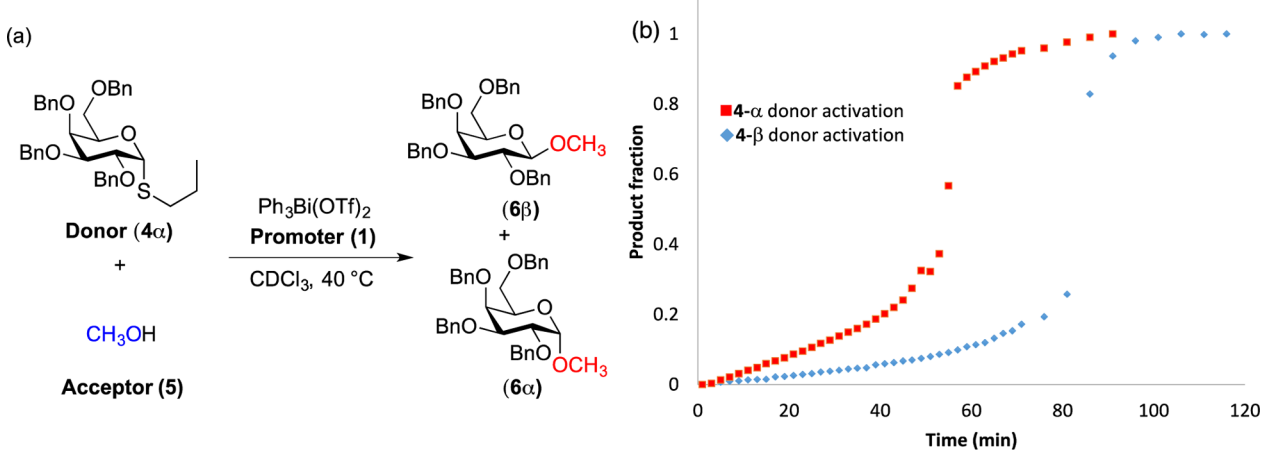

Figure 5. (a) Reaction scheme of **4-α** donor kinetics study; (b) **6-β** product fraction of **4-β** and **4-α** activation vs time. Reaction conditions: (blue diamonds) **4-β**:**1**:**5**::1:1:1 equiv, (red squares) **4-α**:**1**:**5**::1:1:1 equiv, 40 °C, $CDCl_3$.

DOI: 10.1021/acs.joc.6b00860
J. Org. Chem. 2016, 81, 5949−5962

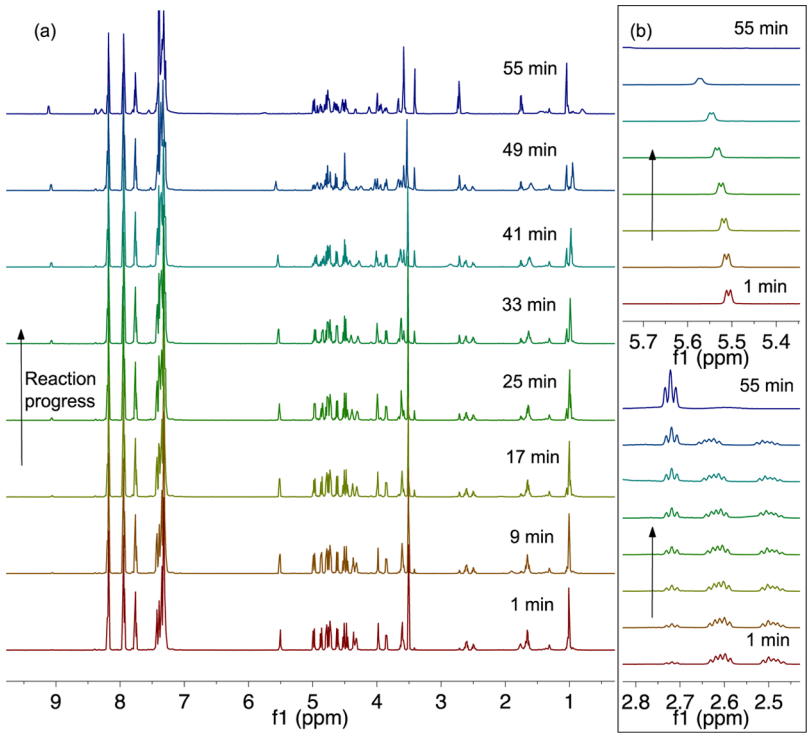

Figure 6. (a) Reaction progress ^{1}H NMR spectrum of the α-donor glycosylation; (b) expanded ^{1}H NMR spectrum showing regions of δ 2.4−2.8 and 5.3−5.8 ppm.

to the glycosyl donor by binding to the thiopropyl arm. As mentioned earlier, another possible mechanism has been proposed by Murphy and co-workers,[49] where it was suggested that a Lewis acidic $TiCl_4$ promoter could chelate to the ring oxygen and a carbonyl group could be installed on the C-6 carbon to form a 5-membered ring, followed by cleavage of the C-1 carbon and the ring oxygen. This method of activation was referred to as endocyclic cleavage. We considered endocyclic cleavage to be a less likely mechanism for anomerization in our system for several reasons. Given that Ti(IV) is an unambiguously hard acid, it is likely that it would prefer coordination to hard bases such as ether oxygens. On the other hand, Bi(V) is a much softer acid and will prefer coordination to a softer base such as a thioether. This is also evident from the observation that the Bi(V) promoter selectively activates only *S*-glycosides in the presence of *O*-glycosides. In addition, the steric strain of trying to insert the much larger bismuth complex **1** into a 5-membered ring will be much worse than for the small $TiCl_4$ complex. Computational results also suggest that endocyclic cleavage is higher in energy (vide infra). We therefore chose to focus on the interaction of Bi(V) with the thioether group.

Because the strength of the Lewis acidity and specific mode of binding will depend on the composition of the Bi(V) promoter, different forms of the promoter must be considered as detailed in Scheme 3. The initial composition of **1** is as a five-coordinate complex, which may lose a triflate ligand to become a cationic four-coordinate species $[Ph_3Bi(OTf)]^+$ (**1a**). Loss of another triflate ligand may afford the dicationic three-coordinate Bi(V) complex $[Ph_3Bi]^{2+}$ (**1b**). As summarized in Scheme 3, dissociation of a triflate ion carries significant energetic penalties of 21.4 and 43.1 kcal/mol, respectively, strongly suggesting that the dominant species in solution is **1**. The presence or release of strong acids such as triflic acid (TfOH) in solution may cause anomerization of glycosides. However, in this case, the high energetics suggests that if in situ generation of TfOH occurs, it is not mediated by the bismuth promoter alone but by its interaction with the substrate(s). Consequently, the most likely reaction scenario is that **1** initially binds to the thiopropyl arm of the sugar.

Scheme 3. Triflate Loss from $Ph_3Bi(OTf)_2$[a]

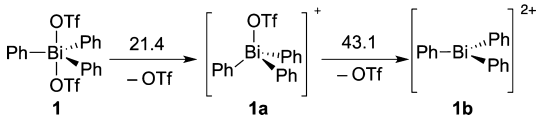

[a]Energies are ΔG(sol) in kcal/mol.

Given the large size and conformational complexity of the thioglycoside itself, we chose to first study how a minimalistic model, Me_2S, binds to bismuth complex **1**. The thioether can either bind at the equatorial or axial positions to afford the octahedral adducts $\mathbf{M1}_{eq}$ or $\mathbf{M1}_{ax}$, respectively (Figure 7). Calculations suggest that $\mathbf{M1}_{eq}$ is unstable and spontaneously loses the thioether ligand, i.e., the six-coordinate geometry is not a minimum on the potential energy surface. Binding thioether in the axial position gives a structure that is a proper minimum, although its formation is uphill by 12.7 kcal/mol on the solution-phase free energy surface. This result is easy to understand; in $\mathbf{M1}_{ax}$, the thioether is in trans disposition to a triflate ligand, whereas in $\mathbf{M1}_{eq}$, the thioether is trans to the much stronger σ-donor phenyl ligand. The strong trans influence of the phenyl ligand weakens the Bi−S bond in $\mathbf{M1}_{eq}$.

Although Me_2S is an adequate general model for the Bi−S bonding, it may not be sufficient for understanding thioglycoside binding to the promoter; the much larger thioglycoside will have significant attractive van der Waals interactions that will assist adduct formation. Indeed, six-coordinate thioglycoside

DOI: 10.1021/acs.joc.6b00860
J. Org. Chem. 2016, 81, 5949−5962

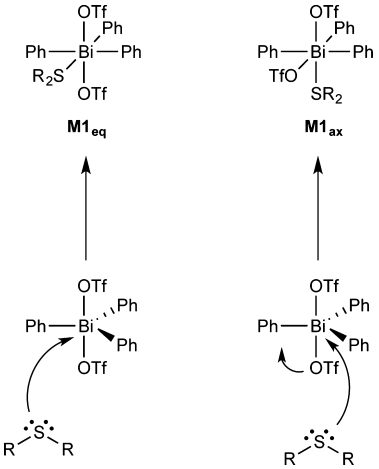

Figure 7. Different relevant binding geometries of an SR_2 ligand to **1**.

adducts for both axial and equatorial binding were located. As expected, the Bi−S distances in the equatorially bound structures were approximately 0.5 Å longer than in the axial bound structures (Table 1). Thus, the Bi−S bond in **9-β_{eq}** and **9-α_{eq}**

Table 1. Calculated Bi−S Bond Lengths for Various Intermediates with the Compound Numbering Presented in Scheme 4

compound	Bi−S length (Å)
$\mathbf{M_{1ax}}$	2.97
9-β_{ax}	2.81
9-α_{ax}	2.89
9-β_{eq}	3.21
9-α_{eq}	3.42
10-β	2.90
10-α	2.94

(see Scheme 4 for compound numbering) is weak if at all existent and is not responsible for binding the thioglycosides; instead, van der Waals interactions are key to maintaining structural integrity. Note that, unless stated otherwise, all calculations use the B3LYP-D3[64−69] functional, which accounts for dispersion interactions. When the geometries of **9-β_{eq}** and **9-α_{eq}** were optimized using the B3LYP functional without Grimme's dispersion corrections, both adducts dissociated into the respective fragments, as seen in the small model. Our decision to use this method is discussed in detail in the Supporting Information.

The energetics of the most relevant intermediates are illustrated in Scheme 4. These calculated energies are valuable information in that they allow us to comment on the thermodynamic viability of proposed reaction pathways. It is important to note that, in the absence of calculated barriers for these steps, we cannot completely validate a proposed reaction step even if it is thermodynamically viable. We do model the barrier heights for oxacarbenium formation, which is discussed in more detail below. For the free thioglycoside, the α-anomer **4-α** was higher in energy than the β-analogue **4-β** by 2.9 kcal/mol. Electronically, the two species were essentially isoenergetic, but entropy corrections give preference to the β-anomer. This result was intriguing as we expected the α-thioglycoside to be more stable than the β-donor owing to the anomeric effect. However, it needs to be noted here that, although the anomeric effect has been observed in some *S*-containing glycosyl donors, extensive high-level calculations have not been done to compute energy differences of α or β donors, especially with the thioglycosides we have chosen to study. Although these calculated anomer energies did not predict the α-thioglycoside to be lower in energy, they do indicate that the two anomers are very close in energy, likely within the error of our computational methodology. This implies that the observed interconversion of donors is possible and that formation of the higher energy α-donor during the reaction is not unreasonable.

Furthermore, binding Bi complex **1** to **4-β** in either axial or equatorial fashion was found to be uphill by 8.2 and 12.4 kcal/mol, respectively. Once bound, the triflate loss was found to be substantially easier, possibly as the Bi center is more electron-rich, and was associated with 1.4 and −2.8 kcal/mol for the axial and equatorial species, respectively. More interestingly, the binding energetics were notably different for **4-α**. Axial binding of **1** was uphill by 9.2 kcal/mol, similar to what was seen for **4-β**, but binding it in the equatorial position was much easier, costing only 0.6 kcal/mol. In other words, formation of the **9-α_{eq}** intermediate via **4-α** or the α-donor requires much less energy than the formation of the other possible intermediates. We suspect that these energy differences may be crucial for determining the reactivities of the donors. At this stage, the triflate loss from the Bi-glycoside complexes are much more favorable. From **9-α**, the release is easy when bound axially (similar to **9-β**) but is more difficult for the equatorially bound structure. In all cases, these energies demonstrate a considerable activation of the Bi complex for triflate loss when compared to free Bi promoter **1** (Scheme 3). Note that additional triflate loss from **10** is difficult (25−30 kcal/mol) and is not considered relevant (see Supporting Information for reaction energies). Altogether, the computed energies for different reaction pathways indicate that formation of a thioglycosyl-bismuthonium-type intermediate is more feasible in an equatorial fashion by the α-donor compared to that of the β-donor, which explains the essential $\beta \rightarrow \alpha$ anomerization. Mechanistically, we have not yet determined how this isomerization of the donors takes place. It is likely, however, that the anomerization is caused by favorable interactions of the *S*-glycoside with the Bi complex and not simply by trace amounts of triflic acid, particularly early on in the mechanism.

As stated earlier, an S_N1-like mechanism involving an oxacarbenium-like intermediate is the accepted mechanism for glycosylation. These glycosyl cations have always been elusive but recently Blériot et al. were able to stabilize these cations in superacid medium and study them by NMR in condensed phase.[70] In our system, the Lewis acidic Bi(V) species can bind to the thiopropyl group, which may make it a better leaving group, and facilitate the oxacarbenium formation. Energetically, it is most reasonable to dissociate the triflate from **9** and abstract the thiolate group, which is associated with modest energies at 8.3 and 6.1 kcal/mol for **10-β** and **10-α**, respectively (Scheme 4). The thiolate abstraction prior to triflate loss was found to be much more demanding thermodynamically and will not be considered further (see Supporting Information for all reaction energetics). Overall, the dissociated five-coordinate $Ph_3Bi(OTf)SPr$ and oxacarbenium intermediate **11** are 17.9 kcal/mol higher in energy than the initial reactants. This is a reasonable energy for a fleeting high-energy intermediate. Our calculations predict that triflate loss from the $Ph_3Bi(OTf)SPr$ species is only uphill by 1.3 kcal/mol.

For **10-β**, an interesting alternative structure labeled as **10-β_{ch}** was found, where the benzyl oxygen on C-6 also coordinates to Bi, essentially allowing the thioglycoside to act as a chelating ligand. At 3.00 Å, the Bi−S bond is lengthened compared to that of **10-β**, and the Bi−O distance is now much shorter

DOI: 10.1021/acs.joc.6b00860
J. Org. Chem. 2016, 81, 5949−5962

Scheme 4. Calculated Energetics of Various Intermediates[a]

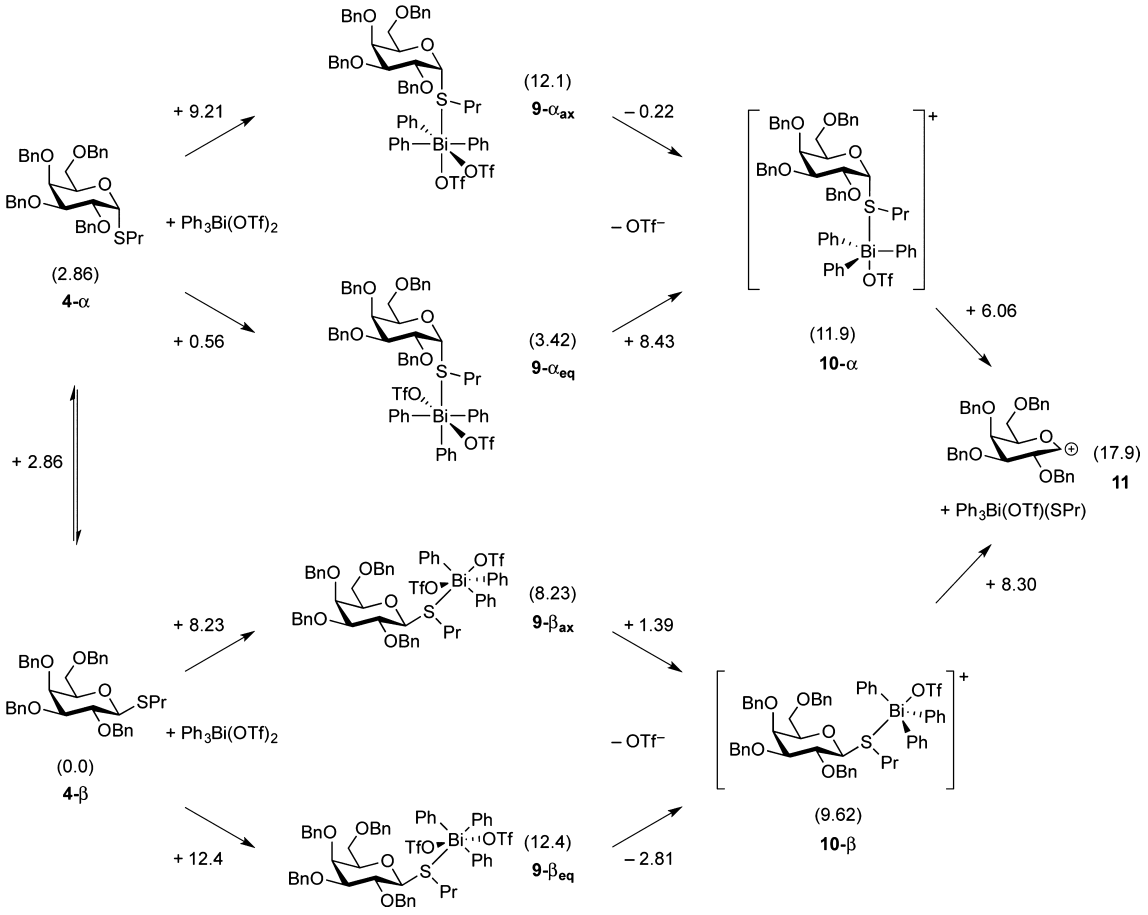

[a]Energies are ΔG(sol) in kcal/mol. Energies in parentheses are relative to **4-*β***.

(3.12 Å reduced from 4.62 Å). In addition, the ring oxygen is also 2.85 Å from Bi, suggesting it may be involved in this coordination as well. These structures are shown in Figure 8.

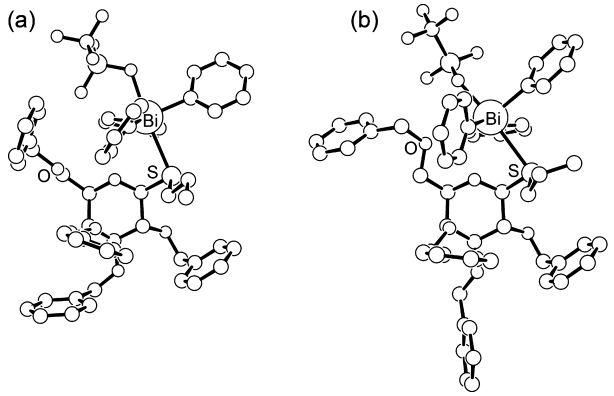

Figure 8. Optimized structures for (a) **10-*β*** and (b) **10-*β*$_{ch}$** with hydrogens omitted for clarity.

This structure was ∼5 kcal/mol higher in energy than **10-*β***, suggesting that this alternative structure may be accessible during the course of the reaction. Although it is not yet clear what, if any, relevance this binding mode might have in the actual chemistry, this unique type of binding was interesting in that it can only occur for the ***β*** form, where the benzyl and sulfur group are on the same side of the ring. It should also be noted that this structure is somewhat reminiscent of the chelate structure proposed by Murphy discussed earlier. Notably, however, the primary interaction is still with the sulfur atom and not constrained to form a five-membered ring with the two oxygen bases. This suggests that activation at the sulfur arm will still be possible, if not preferred. Although we did not extensively probe the endocyclic cleavage mechanism, we did use DFT to probe the stability of the critical 6-coordinate intermediate (**10**$_{En}$). As shown in Scheme 5, this structure is 9.29 kcal/mol higher in solvated free energy than $Ph_3Bi(OTf)SPr$ and **11**. This suggests that, even if endocyclic cleavage did occur, forming an oxacarbenium ion will still be the most likely energetic path.

Assuming that thiolate abstraction from **10** is the most relevant for oxacarbenium formation, we modeled the barrier for this process by performing a relaxed scan (Figure 10) along the C−S distance for **10-*β***, and **10-*α***. These scans did not yield genuine S_N1 transition states but they provided an upper-limit estimate for the barrier height for these pathways. The points along the trajectories (Figure 9) are located by constrained optimizations and hence entropic and zero point energy (ZPE) corrections are not meaningful. These scans show a sharp initial increase in energy corresponding to breaking the C−S bond. Instead of decreasing at larger C−S distances, the energy levels off and or gently increases. Thus, electronically, there is no saddle point that would correspond to a transition state. At long C−S distances, the α and β trajectories have similar energies, especially when solvation corrections are added, which considerably lower the energy at these distances due to growing charge separation in

DOI: 10.1021/acs.joc.6b00860
J. Org. Chem. 2016, 81, 5949−5962

Scheme 5. Depiction of Endocyclic Cleavage from 10-β[a]

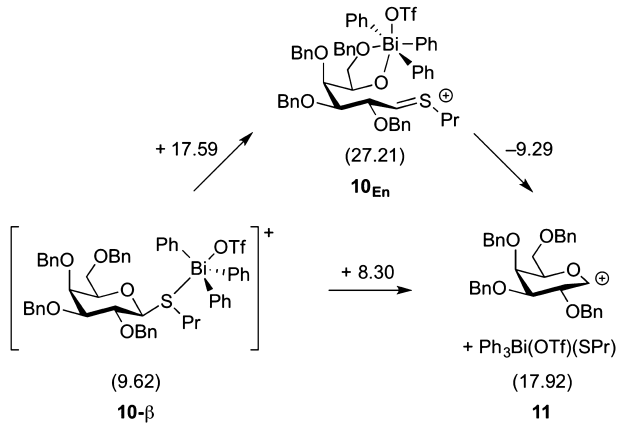

[a]Energies are ΔG(sol) in kcal/mol. Energies in parentheses are relative to **4-β**.

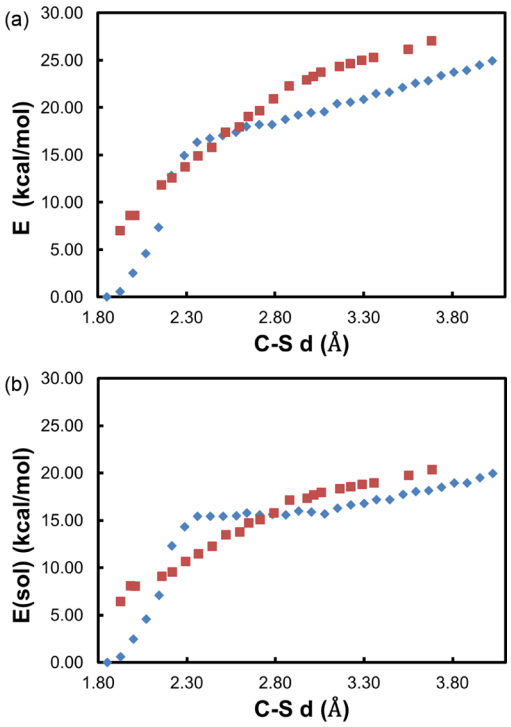

Figure 9. (a) Electronic energies of **10** as a function of C−S distance; (b) E(sol) (electronic energies with solvation corrections) of **10** as a function of C−S distance. The β anomer is represented with blue diamonds, and α is represented with red squares.

the dissociating fragments. These energies at long distances can be used to estimate the barriers to be ∼18 and ∼14 kcal/mol for **10-β** and **10-α**, respectively. Because **10-β** and **10-α** are 9.6 and 11.8 kcal/mol higher in energy than the reactants, as illustrated in Scheme 4, the overall reaction barriers can be estimated to be ∼28 and ∼26 kcal/mol for **10-β** and **10-α**, respectively. These energies are referenced to **4-β**, and because **4-α** is 2.9 kcal/mol higher in energy than **4-β**, the reaction may be more facile when starting directly from **4-α**. The estimated barrier heights are reasonable for a reaction that proceeds slowly at 40 °C, and these calculations suggest that oxacarbenium formation is consistent with the time scale of the reaction. In addition, given that the reverse reaction(s) will be substantially faster, this also offers a reasonable pathway for anomerization to either **4-α** or **9-α** when it is equatorially bound.

A final comment is necessary regarding the quality of our computational results and methodology. Given the challenges in both properly searching the conformational space and in accurately modeling the delicate nonbonding energetics (both of which are discussed in the Supporting Information), the results here should be interpreted appropriately. It is not our intent to propose that we have necessarily located the absolute lowest energy structures (global minima) for every possible species, nor that we have definitively found the only possible mechanisms of anomerization. Rather, we present a thorough DFT study that demonstrates the kinetic and thermodynamic viability of our proposed mechanism and complex speciation within the level of accuracy and precision afforded to us by present-day computational methodologies.

With the computational evidence for the favorable formation of a Bi-glycosyl sulfonium species, we chose to investigate these ions further with NMR spectroscopy. Glycosyl sulfonium species have been extensively studied previously,[71] and although notoriously unstable, they have been isolated and studied by NMR.[31,72] Most of these studies are on β-glycosyl sulfonium species,[71] except a report by Yoshida et al. on the generation and reactivity of α- and β-glucosyl sulfonium ions.[42] Curiously, they found that the α-sulfonium species reacted faster than their β-counterparts and attributed this to the distortion of the tetrahydropyran ring of the activated species. This outcome complements our observations that the β-donor converts to the α-donor as it presumably forms a much more reactive sulfonium. As observed in the ^{1}H NMR kinetic studies of the **4-α** donor, the H-1 doublet peak shape and chemical shift changes (Figure 6b) are indicative of a reactive intermediate, and to analyze it, we performed a variety of 1D and 2D NMR experiments. These experiments were done at various stages of both donor **4-α/β** activation with the Bi(V) promoter without any acceptor in $CDCl_3$ at different temperatures. Unfortunately, our efforts to obtain structural information on the intermediate by through bond-based (HSQC, HMBC, COSY, TOCSY) and diffusion-based (DOSY) NMR approaches were not successful. Correlations of the reactant **4-β** protons with sugar ring carbons and the promoter protons with phenyl ring carbons could be seen throughout the reaction, but correlations between the donor and promoter were not detected. It needs to be pointed out here that, although sulfonium species have been well-studied, glycosyl sulfonium species connected to Bi or any other heavy-metal atoms have not been reported or studied by NMR earlier.

The other strategy that we attempted to gain evidence for the formation of a Bi-glycosyl sulfonium species was application of through space-based (NOESY, ROESY) NMR spectroscopy. Fortunately, the 1D-selective NOE studies, where the peaks of interest can be irradiated to show correlations to other peaks, proved to be informative, although the 2D NOE experiments failed to show interesting peaks. As shown in Figure 10(b), when CH_3 (1.0 ppm) of the thiopropyl group was irradiated, it correlated with the Ph protons on **1**; in (c), CH_2 on the thiopropyl group (2.6 ppm) upon irradiaton surprisingly showed strong correlation signals with the phenyl protons but weak signals with the rest of the thiopropyl protons. In (d), when the transient H-1 peak on the thioglycoside was irradiated (5.5 ppm), it correlated with the Ph protons on **1** as well as other sugar ring protons; in (e), when the in situ generated peak (9.2 ppm) belonging to an activated PhBi species was selectively irradiated, it correlated with peaks on the glycoside, specifically the methyl

DOI: 10.1021/acs.joc.6b00860
J. Org. Chem. 2016, 81, 5949−5962

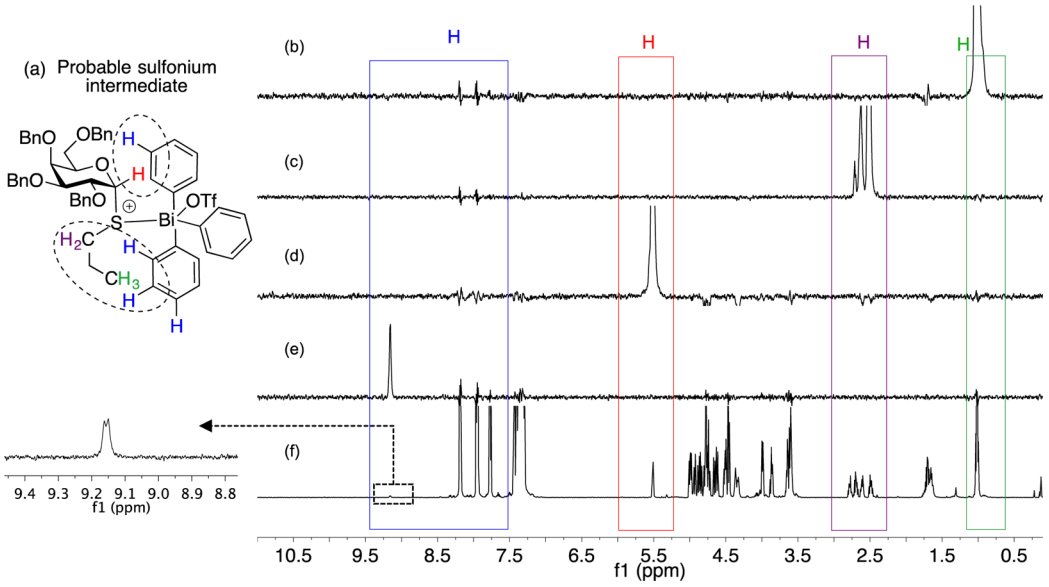

Figure 10. (a) Structure of probable intermediate; 1D selective NOESY of peaks at chemical shifts of δ (b) 1.0, (c) 2.6, (d) 5.5, and (e) 9.2 ppm showing correlation with other peaks; (f) ^{1}HNMR of the activation shown in Figure 4a.

(CH_3). On the basis of these interactions, the Bi-sulfonium intermediate generated by the computational studies appears to be reasonable [Figure 10(a)]. For example, the thiopropyl arm of the glycoside is more flexible, and hence, the terminal CH_3 (1.0 ppm) can have more spatial interactions with the phenyl protons on **1**. Similarly, the new Ph proton peak (9.2 ppm) on the Bi species correlated with this CH_3 peak. Interestingly, when the original Ph peaks on **1** (δ 7.7−8.2 ppm) were selected, they failed to correlate to any peaks on the glycoside except each other. This suggests that when **1** binds or is modified, new peaks corresponding to some of these protons were created, which can be seen in the 7−9.5 ppm region. These interactions showcase some structural assignments, but more studies are required to definitively confirm the Bi-sulfonium species.

To gain more insight into the anomerization of donors, we were curious if the presence of a coordinating group like an acetate at the C-2 position of the thioglycosyl donor would hinder this isomerization. As mentioned above, certain functional groups at the C-2 position of the glycosyl donor can direct the stereochemistry and afford 1,2 *trans* products exclusively. It has been shown that the carboxyl oxygen of the ester on the C-2 group can form a transient, bridged dioxalenium ion with the anomeric carbon.[73−75] In this putative intermediate, the attack of a nucleophile from the "bottom side of the molecule", i.e., the α-face of the glycosyl donor, becomes difficult. Hence, the incoming nucleophile attacks preferentially from the equatorial or the β-face resulting in the 1,2 *trans* diastereomers. In our experiments so far, we observed the $\beta \rightarrow \alpha$ isomerization when a nonparticipating group or a benzyl ether was present at the neighboring C-2 position of the β-thioglycoside. For this hypothesis to be tested, the α- and β-3,4,6-*O*-benzyl 2-*O*-acetate thiopropyl galactoside (**7-α/β**) donors were prepared. This thioglycoside donor was chosen as it is a galactoside donor like **4-α/β**, and the functional groups present are identical to **4-α/β** except at the C-2 position. These type of donors containing electron-rich benzyl groups (Bn) on the C-3,4,6 positions and a participating group at the C-2 position (like acetates, benzoates, etc.) have previously been found to be highly reactive substrates and are generally labeled as superarmed donors.[76]

The glycosylation of donor **7-β** was carried out with methanol (**5**) in the presence of promoter **1** (Figure 11a). The reaction

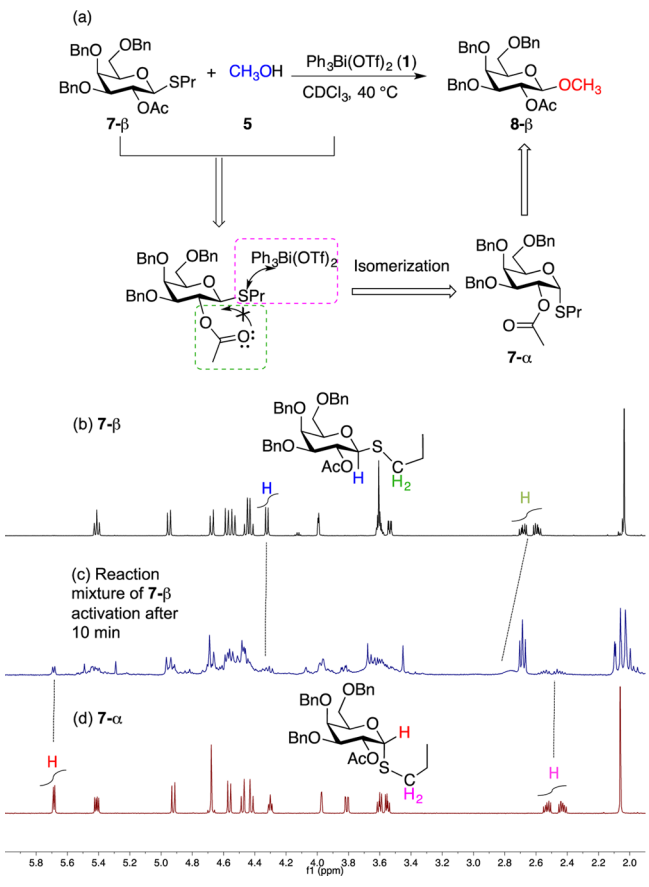

Figure 11. (a) Scheme of superarmed β-donor activation (**7-β**); ^{1}H NMR comparison of the activation; (b) ^{1}H NMR β-donor (**7-β**); (c) reaction mixture ^{1}H NMR of activation of **7-β** after 10 min; and (d) ^{1}H NMR of the α-donor (**7-α**).

DOI: 10.1021/acs.joc.6b00860
J. Org. Chem. 2016, 81, 5949−5962

was relatively fast, reaching completion within 20 min, in contrast to the activation of donor **4-β**, which required 101 min for complete reaction. The ^{1}H NMR spectra of the pure anomers (Figure 11b,d) were compared to the ^{1}H NMR of a reaction mixture (Figure 7c). Correlating the peaks in the region of 2.2−6.0 ppm, where most carbohydrate signals appear, some common characteristic peaks were observed as shown by dotted lines in Figure 11. Figure 11c shows a doublet at δ = 4.32 ppm (J = 9.9 Hz) and a multiplet at δ = 2.7 ppm, which correspond to the H-1 and the CH_2 of the beta-donor **7-β**. Apart from these peaks, another doublet at δ = 5.69 ppm (J = 5.6 Hz) can be seen in the reaction mixture, which corresponds to the H-1 peak of the alpha-donor **7-α** and therefore indicates that this donor is present in the reaction mixture. In addition, another multiplet at δ = 2.4 ppm assigned to the CH_2 protons of the α-donor was seen to appear as the reaction progressed. These observations support the conclusion that the β anomer **7-β** isomerizes to the α anomer **7-α** during the activation. In addition to NMR evidence, thin layer chromatography (TLC) taken during the activation also showed the appearance of the α-donor **7-α** along with the β-donor **7-β** spot (both have distinct R_fs) as the reaction progressed. Taken together, this evidence suggests that the presence of a coordinating acetate group at the C-2 position does not preclude the $\beta \rightarrow \alpha$ anomerization of the superarmed thioglycosyl donor during its activation by a Bi(V) promoter. Interestingly, the *O*-methyl glycoside obtained at the end of the **7-β** activation was found to be exclusively the 1,2-*trans* isomer (α/β = 1:20), which is in stark contrast to no stereoselectivity (α/β = 1:1) obtained with **4-β** activation. This result suggests that, although the acetate group at C-2 does not hinder the in situ anomerization, it plays a crucial role in the stereochemical outcome of the activation.

CONCLUSIONS

In summary, the first mechanistic studies of $Ph_3Bi(OTf)_2$-mediated thiopropylglycoside activation have revealed an unprecedented anomerization of the β-donor to the α-analogue as an essential step during the glycosylation. As a consequence, use of the α-donor alone gave rise to better product stereoselectivity and increased reaction speeds, thereby addressing some of the practical goals for these mechanistic studies. Interestingly, both donors followed a sigmoidal-type kinetics pathway consisting of an initial slow promoter activation step. Computational analysis delineated the most likely intermediates involved in activating the thioglycoside, including showing that a penta- rather than tetra-coordinate bismuth species is most likely to coordinate to the sulfur of the thioglycoside initially and that oxacarbenium formation mediated by $Ph_3Bi(OTf)_2$ was viable and in the energy range expected based on experimental conditions. In addition, we found that the α-thioglycoside was effectively equal in energy to the β-form when entropy terms were ignored. As the calculations did not completely explain the necessary isomerization of the β- to α-donor during activation or the observed rate acceleration with the α-anomer, it suggests that this effect may be related to the formation of favorable α- versus β-glycosyl sulfonium-bismuth intermediates. The oxacarbenium formation mechanism was also investigated but did not provide us with information about the observed reactivity of the donors. Some preliminary insights into the bismuth-sulfonium complex were obtained with NOE NMR studies, and this data supports the existence of the computationally generated reactive intermediates. Moreover, the β- to α-anomerization reaction could still be seen with the superarmed donor, i.e., in the presence of NGP by a C-2 acetate group. Although these studies obviously cannot settle every question as to how thioglycoside reactions work and how Bi(V) species operate, they serve as a good foundation for future experiments and computational work in this area.

EXPERIMENTAL SECTION

General Experimental. All reactions were carried out in oven- or flame-dried glassware, septum-capped under atmospheric pressure of argon using anhydrous solvents unless otherwise stated. Air- and moisture-sensitive liquids and solutions were transferred via syringe or stainless steel cannula. Solvents used in the reactions were obtained from a solvent purification system having an alumina-packed column. For the kinetic experiments, methanol and d_1-chloroform were distilled and kept over 3 Å molecular sieves. All saccharides were predried by azeotropic removal of water using toluene. Prior to use and to ensure dryness, $Ph_3Bi(OTf)_2$ was kept in a vacuum desiccator containing P_2O_5 overnight. Analytical thin-layer chromatography (TLC) plates were detected under UV light or by spraying the plates with a 0.02 M solution of resorcinol in 20% ethanolic H_2SO_4 solution followed by heating. Proton (^{1}H) NMR, carbon (^{13}C) NMR, and 2D NMR were recorded using the residual signals from d_1-chloroform ($CDCl_3$), δ 7.26 and 77.0 ppm, as internal references for ^{1}H and ^{13}C chemical shifts (δ), respectively.

Syntheses of Compounds. *n-Propyl-2,3,4,6-tetra-O-benzyl-1-thio-β-D-galactopyranoside (4-β).*

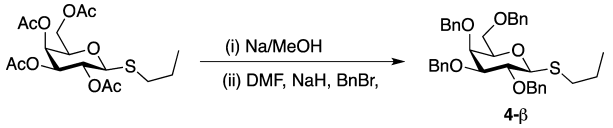

4-β

Glycosyl donor was converted to thiopropylgalactoside (**4-β**) following reported methods. The ^{1}H and ^{13}C NMR spectral data matched with literature.[21]

n-Propyl-2,3,4,6-tetra-O-benzyl-1-thio-α-D-galactopyranoside (4-α).

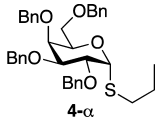

4-α

During the preparation of the beta galactoside donor (**4-β**), the alpha galactoside donor (**4-α**) was obtained as a minor product. The compound is a pale yellow oil; R_f = 0.62 (ethyl acetate:hexanes, 1:5); $[\alpha]_D$ +83.4 cm^3 g^{-1} dm^{-1} (c 0.14 g cm^{-3}, $CHCl_3$); ^{1}H NMR (400 MHz, [D-1] $CDCl_3$, 25 °C, TMS) δ 7.42−7.27 (m, 20H; $\underline{Ph}CH_2O$), 5.46 (d, J = 5.5 Hz, 1H; H-1), 4.95 (d, J = 11.4 Hz), 4.84 (d, J = 11.8 Hz), 4.75 (d, J = 11.7 Hz), 4.72−4.66 (m), 4.59−4.55 (m), 4.49−4.37 (m) [8H, $PhC\underline{H}_2O$], 4.33−4.29 (m), 4.29−4.25 (m), 3.93 (d, J = 2.4 Hz), 3.81 (dd, J = 9.9, 2.9 Hz) [4H, H-2,3,4,5], 3.54 (d, J = 6.4 Hz, 2H, H-6ab), 2.61−2.39 (m, 2H, $SC\underline{H}_2CH_2CH_3$), 1.65−1.58 (m, 2H, $SCH_2C\underline{H}_2CH_3$), 0.97 (t, J = 7.3 Hz, 3H, $SCH_2CH_2C\underline{H}_3$); ^{13}C NMR (151 MHz, [D-1] $CDCl_3$, 25 °C, TMS) δ 138.91, 138.75, 138.39, 138.18 (4C, 4 × C-1′ C_{Ph}), 128.4, 128.4, 128.4, 128.3, 128.3, 128.0, 127.7, 127.7, 127.6, 127.6, 127.5 (20C, C_{Ph}), 83.8 (1C; C-1), 79.7, 76.4, 75.3 (3C, C-2,3,4), 74.9, 73.5, 73.5, 72.6 (4C, $Ph\underline{C}H_2O$), 69.8 (1C, C-5), 69.2 (1C,C-6), 31.6 (1C, $S\underline{C}H_2CH_2CH_3$), 22.9 (1C, $SCH_2\underline{C}H_2CH_3$), 13.7 (1C, $SCH_2CH_2\underline{C}H_3$); HRMS (ESI-QTOF) m/z calcd for $C_{37}H_{42}O_5$ SEt_3NH^+ 700.4035, found 700.4031; m/z calcd for $C_{37}H_{42}O_5SNa^+$ 621.2645, found 621.2641.

Triphenyl Bismuth Ditriflate (1).

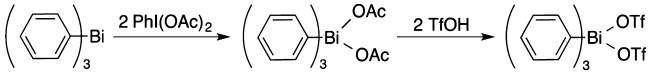

5

Promoter (**1**) was prepared by following a procedure previously developed in our lab.[21]

DOI: 10.1021/acs.joc.6b00860
J. Org. Chem. 2016, 81, 5949−5962

Table 2. Time Points of Data Acquisition for Reaction Kinetics Experiments

FID #	time (min)	FID #	time (min)	FID #	time (min)	FID #	time (min)	FID #	time (min)
1	1	17	33	33	65	49	136	65	216
2	3	18	35	34	67	50	141	66	221
3	5	19	37	35	69	51	146	67	226
4	7	20	39	36	71	52	151	68	231
5	9	21	41	37	76	53	156	69	236
6	11	22	43	38	81	54	161	70	241
7	13	23	45	39	86	55	166	71	246
8	15	24	47	40	91	56	171	72	251
9	17	25	49	41	96	57	176	73	256
10	19	26	51	42	101	58	181	74	261
11	21	27	53	43	106	59	186	75	266
12	23	28	55	44	111	60	191	76	271
13	25	29	57	45	116	61	196	77	276
14	27	30	59	46	121	62	201	78	281
15	29	31	61	47	126	63	206	79	286
16	31	32	63	48	131	64	211	80	290

*n-Propyl-2-O-acetyl-3,4,6-tetra-O-benzyl-1-thio-D-galactopyranoside (**7-β, 7-α**).*

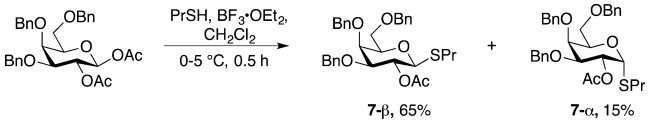

A 0.50 M solution of glycosyl acetate donor[77] (1.50 g, 2.81 mmol) and propanethiol (PrSH, 0.256 g, 3.37 mmol) was stirred for 0.5 h in anhydrous dichloromethane at 0 °C. Then, boron trifluoride diethyerate (BF_3·OEt_2, 1.19 g, 8.42 mmol) was added dropwise to the reaction mixture, and it was stirred over an ice bath (0−5 °C) until consumption of the starting donor was seen by TLC. The reaction was quenched with excess triethylamine, diluted with CH_2Cl_2, filtered, and washed sequentially with 2 M aqueous HCl, saturated aqueous $NaHCO_3$, and water. The organic layer was dried over $MgSO_4$ and concentrated under reduced pressure at 40 °C, and the resulting residue was purified by silica gel column chromatography by a solvent system (ethyl acetate:hexanes, 1:7), which yielded the following:

Compound (**7-*β***) as a white amorphous solid (0.99 g, 65%); R_f = 0.65 (ethyl acetate:hexanes, 1:4); $[\alpha]_D$ +67.3 cm^3 g^{-1} dm^{-1} (*c* 0.12 g cm^{-3}, $CHCl_3$); ^{1}H NMR (600 MHz, [D-1] $CDCl_3$, 25 °C, TMS) 7.31 (m, 15 H, $\underline{Ph}CH_2O$) 5.41 (t, *J* = 9.7 Hz, 1H, H-2), [4.95 (d, *J* = 11.7 Hz), 4.68 (d, *J* = 12.2 Hz), 4.58−4.55 (2 d, *J* = 11.9 Hz), 4.48−4.39 (m)] (6H, 6 × $PhC\underline{H}_2O$), 4.32 (d, *J* = 9.9 Hz, 1H, H-1), 3.99 (dd, *J* = 2.8, 0.9 Hz, 1H, H-4), 3.62−3.57 (m, 3H, H-5,H-6ab), 3.54 (dd, *J* = 9.7, 2.8 Hz, 1H, H-3), 2.64 (dddd, *J* = 12.4, 8.3, 6.5 Hz, 2H, $SC\underline{H}_2CH_2CH_3$), 2.04 (s, 3H, $C\underline{H}_3C$ = O) 1.64−1.56 (m, 2H, $SCH_2C\underline{H}_2CH_3$), 0.94 (t, *J* = 7.4 Hz, 3H, $SCH_2CH_2C\underline{H}_3$); ^{13}C NMR (151 MHz, $CDCl_3$) *δ* 169.8, 138.7, 138.1, 137.9, 128.5, 128.5, 128.3, 128.1, 128.0, 127.9, 127.8, 127.6, 127.5, 83.9, 81.6, 77.6, 77.4, 77.2, 76.9, 74.5, 73.7, 73.0, 72.1, 69.8, 68.7, 31.7, 23.2, 21.2, 13.6; HRMS (ESI-QTOF) *m*/*z* calcd for $C_{32}H_{38}O_6SNa^+$ 573.2286, found 573.2291.

Compound (**7-*α***) as a clear syrup (0.23 g, 15%); R_f = 0.72 (ethyl acetate:hexanes, 1:4); $[\alpha]_D$ +67.3 cm^3 g^{-1} dm^{-1} (*c* 0.12 g cm^{-3}, $CHCl_3$); ^{1}H NMR (600 MHz, [D-1] $CDCl_3$, 25 °C, TMS) *δ* 7.36−7.27 (m, 15H, $\underline{Ph}CH_2O$), 5.69 (d, *J* = 5.6 Hz, 1H, H-1), 5.41 (dd, *J* = 10.3, 5.7 Hz, 1H, H-2), [4.92 (d, *J* = 11.5 Hz), 4.68 (s), 4.56 (d, *J* = 11.5 Hz), 4.48 (d, *J* = 11.8 Hz), 4.42 (d, *J* = 11.7 Hz), (6H, 6 × $PhC\underline{H}_2O$)], 4.30 (t, *J* = 6.5 Hz, 1H, H-4), 3.97 (d, *J* = 3.0 Hz, 1H, H-4), 3.81 (dd, *J* = 10.3, 2.9 Hz, 1H, H-3), 3.62−3.53 (m, 2H, H, H-6ab), 2.48 (dddd, *J* = 12.8, 8.1, 6.6 Hz, 2H $SC\underline{H}_2CH_2CH_3$), 2.06 (s, 3H, $C\underline{H}_3C$═O), 1.63−1.56 (m, 2H, $SCH_2C\underline{H}_2CH_3$), 0.93 (t, *J* = 7.3 Hz, 3H, $SCH_2CH_2C\underline{H}_3$); ^{13}C NMR (151 MHz, $CDCl_3$) *δ* 170.3, 138.6, 138.4, 138.1, 128.5, 128.5, 128.4, 128.3, 127.8, 127.7, 127.5, 82.5, 77.7, 77.2, 74.9, 74.7, 73.6, 73.0, 71.4, 69.7, 68.9, 32.1, 23.0, 21.2, 13.6; HRMS (ESI-QTOF) *m*/*z* calcd for $C_{32}H_{38}O_6SNa^+$ 573.2287, found 573.2284.

Kinetics Experimental Data. Various temperatures were tried for monitoring the reaction kinetics, and out of these, 40 °C (313 K) was found to be the optimum temperature considering the total reaction time. NMR tubes were flame-dried before use.

Typical Procedure. The glycosyl donor (1 equiv, 0.025 mmol) and promoter (1 equiv, 0.025 mmol) were weighed in a septum-capped oven-dried 1-dram vial, purged with argon, and then taken to the NMR instrument. The thermostat of the NMR instrument was allowed to stabilize at 313 K. Then, the instrument was locked and shimmed using an NMR tube containing only $CDCl_3$. A stock solution of the acceptor, MeOH in deuterated $CDCl_3$, was prepared, and then the required amount (1 equiv, 0.025 mmol) was added to the vial via a syringe. The total volume of the solvent was kept constant for each experiment (0.6 mL). The vial was shaken until the reaction mixture reached homogeneity (generally ∼5−7 s), transferred to a new flame-dried NMR tube, and immediately inserted into an NMR machine for data acquisition. This was taken as time zero, and automatic spectra of 4 scans with a 24 s acquisition delay (D1) between scans were registered automatically every 120 s for the first 69 FIDs, after which scans were taken at intervals of 300 s (Table 2). The spectra obtained were processed manually to obtain the concentration of reactant and product species during the experiment.

Radical Mechanism Studies with Scavengers. (a) For the NMR reaction monitoring, we followed the same protocol as described

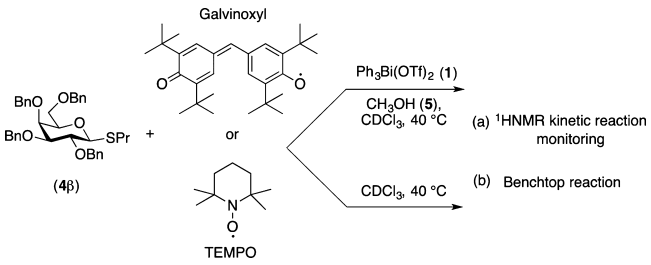

above. The amounts of the reactants were donor **4*β*** (1 equiv, 15.0 mg, 0.025 mmol), promoter **1** (1 equiv, 18.0 mg, 0.025 mmol), scavenger (1 equiv, 0.025 mmol), and MeOH (1 equiv, 0.001 mL, 0.025 mmol). The scavenger was added along with MeOH in $CDCl_3$. For these experiments, special care was taken to degas the solvents before use, which was done by three freeze−pump−thaw cycles. The reaction was then monitored by NMR.

(b) For benchtop reaction monitoring, the donor **4*β*** (1 equiv, 15.0 mg, 0.025 mmol) and promoter **1** (1 equiv, 18.0 mg, 0.025 mmol) were taken in a dry 10 mL round-bottomed flask under Ar. To the flask was added a solution of MeOH (1 equiv, 0.001 mL, 0.025 mmol) and scavenger (1 equiv, 0.025 mmol) in $CDCl_3$. The progress of the reaction

DOI: 10.1021/acs.joc.6b00860
J. Org. Chem. 2016, 81, 5949−5962

Table 3. Analyte Analysis

analyte	formula	mw	rt (min)	peak height	peak area	density	stock concn	RRF
PrSH	C_3H_8S	76	2.124	870	21.54	0.84	42	3.375
PrSSPr	$C_6H_{14}S_2$	150	8.166	1680	34.37	0.96	48	4.471
Dodecane	$C_{12}H_{26}$	170	9.092	271	5.69	0.75	37.45	1.000
PhSPr	$C_9H_{12}S$	152	9.575	2449	54.06	0.99	50	7.116

or consumption of the donor/formation of products was then monitored by TLC.

Both the NMR and benchtop reaction monitoring were done in absence of promoter as control studies to rule out any interfering effects by the scavengers on the reactants.

GC-MS Studies. *Materials.* PrSH was commercially bought and distilled before use. PrSSPr and PhSPr[46] were synthesized following literature methods and distilled before use.

Procedure for Separation of Analytes. For the retention times of the analytes to be determined, stock solutions were prepared by mixing 1 μL of each of the analytes, PrSH, PrSSPr, PhSPr, and an internal standard (dodecane), in 100 mL of CH_2Cl_2 and analyzing them on the GC-MS instrument. The retention times were recorded, and the relative response factors (RRF) were then calculated. All of the analytes were separated on the chromatogram and could be monitored (Table 3).

General Procedure of Reaction Monitoring by GC-MS.

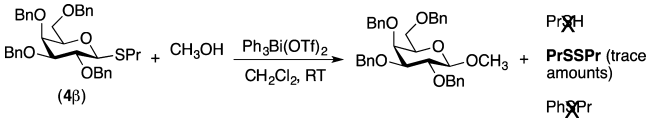

The glycosyl donor (1 equiv, 0.033 mmol, 20.0 mg) and promoter (1 equiv, 0.033 mmol, 25.0 mg) were taken in a tightly sealed oven-dried flask under Ar. To it was added a solution of MeOH (1 equiv, 0.033 mmol, 1.35 μL) in CH_2Cl_2, and the reaction was left to stir under argon. Aliquots (1 μL) from the reaction mixture at various times were then taken out, mixed with dodecane to make 50 mL stock solutions in CH_2Cl_2, and then immediately analyzed by GC-MS. The donor consumption was also monitored by TLC. Note: Only trace amounts of PrSSPr were observed at the end of the glycosylation (see GC-MS spectra T = 1 h in the Supporting Information).

■ ASSOCIATED CONTENT

Supporting Information

The Supporting Information is available free of charge on the ACS Publications website at DOI: 10.1021/acs.joc.6b00860.

1D and 2D NMR spectra of compounds **4a**, **7a**, and **7b**, reaction kinetics NMR and GC spectra, and computational methodologies and calculations (PDF)

■ AUTHOR INFORMATION

Corresponding Authors

*E-mail: mbaik2805@kaist.ac.kr.

*E-mail: npohl@indiana.edu.

Notes

The authors declare no competing financial interest.

■ ACKNOWLEDGMENTS

This material is based in part upon work supported by the National Science Foundation under CHE-1362213. Purchase of the AVIII-600 NMR spectrometer used to obtain results included herein was supported by the National Science Foundation under Grant No. MRI 1040098. We thank the Institute for Basic Science in Korea for partial support of this work (IBS-R10-D1).

■ REFERENCES

(1) Bertozzi, C. R.; Kiessling, L. L. *Science* **2001**, *291*, 2357.
(2) Varki, A. *Essentials of Glycobiology*, 2nd ed., 2009.
(3) DeMarco, M. L.; Woods, R. J. *Glycobiology* **2008**, *18*, 426.
(4) Werz, D. B.; Seeberger, P. H. *Chem. - Eur. J.* **2005**, *11*, 3194.
(5) Dwek, R. A.; Butters, T. D.; Platt, F. M.; Zitzmann, N. *Nat. Rev. Drug Discovery* **2002**, *1*, 65.
(6) Kahne, D.; Leimkuhler, C.; Lu, W.; Walsh, C. *Chem. Rev.* **2005**, *105*, 425.
(7) Prassas, I.; Diamandis, E. P. *Nat. Rev. Drug Discovery* **2008**, *7*, 926.
(8) Nigudkar, S. S.; Demchenko, A. V. *Chem. Sci.* **2015**, *6*, 2687.
(9) Boltje, T. J.; Buskas, T.; Boons, G.-J. *Nat. Chem.* **2009**, *1*, 611.
(10) Demchenko, A. V. In *Handbook of Chemical Glycosylation*; Wiley-VCH Verlag GmbH & Co. KGaA, 2008; p 1.
(11) Nicolaou, K. C.; Mitchell, H. J. *Angew. Chem., Int. Ed.* **2001**, *40*, 1576.
(12) Kim, J.-H.; Yang, H.; Park, J.; Boons, G.-J. *J. Am. Chem. Soc.* **2005**, *127*, 12090.
(13) Zhu, X.; Schmidt, R. R. *Angew. Chem., Int. Ed.* **2009**, *48*, 1900.
(14) Whitfield, D. *Adv. Carbohydr. Chem. Biochem.* **2009**, *62*, 83.
(15) Hosoya, T.; Takano, T.; Kosma, P.; Rosenau, T. *J. Org. Chem.* **2014**, *79*, 7889.
(16) Mydock, L. K.; Demchenko, A. V. *Org. Biomol. Chem.* **2010**, *8*, 497.
(17) Ranade, S. C.; Demchenko, A. V. *J. Carbohydr. Chem.* **2013**, *32*, 1.
(18) Frihed, T. G.; Bols, M.; Pedersen, C. M. *Chem. Rev.* **2015**, *115*, 4963.
(19) Whitfield, D. *Adv. Carbohydr. Chem. Biochem.* **2009**, *62*, 83.
(20) Crich, D. *Acc. Chem. Res.* **2010**, *43*, 1144.
(21) Goswami, M.; Ellern, A.; Pohl, N. L. B. *Angew. Chem., Int. Ed.* **2013**, *52*, 8441.
(22) Barton, D. H. R.; Bhatnagar, N. Y.; Finet, J.-P.; Motherwell, W. B. *Tetrahedron* **1986**, *42*, 3111.
(23) Barton, D. H. R.; Kitchin, J. P.; Lester, D. J.; Motherwell, W. B.; Papoula, M. T. B. *Tetrahedron* **1981**, *37*, 73.
(24) Matano, Y. In *Bismuth-Mediated Organic Reactions*; Ollevier, T., Ed.; Springer: Berlin Heidelberg, 2012; Vol. *311*, p 19.
(25) Matano, Y.; Ikegami, T. In *Organobismuth Chemistry*; Suzuki, H., Matano, Y., Eds.; Elsevier Science: Amsterdam, 2001; p 247.
(26) Ollevier, T. *Org. Biomol. Chem.* **2013**, *11*, 2740.
(27) Bothwell, J. M.; Krabbe, S. W.; Mohan, R. S. *Chem. Soc. Rev.* **2011**, *40*, 4649.
(28) Adams, J. R.; Goswami, M.; Pohl, N. L. B.; Mallapragada, S. K. *RSC Adv.* **2014**, *4*, 15655.
(29) Park, J.; Kawatkar, S.; Kim, J.-H.; Boons, G.-J. *Org. Lett.* **2007**, *9*, 1959.
(30) Fang, T.; Mo, K.-F.; Boons, G.-J. *J. Am. Chem. Soc.* **2012**, *134*, 7545.
(31) Mydock, L. K.; Kamat, M. N.; Demchenko, A. V. *Org. Lett.* **2011**, *13*, 2928.
(32) Bunton, C. A.; Lewis, T. A.; Llewellyn, D. R.; Vernon, C. A. *J. Chem. Soc.* **1955**, *0*, 4419.
(33) Rhind-Tutt, A. J.; Vernon, C. A. *J. Chem. Soc.* **1960**, 4637.
(34) Armour, C.; Bunton, C. A.; Patai, S.; Selman, L. H.; Vernon, C. A. *J. Chem. Soc.* **1961**, *0*, 412.
(35) Banks, B. E. C.; Meinwald, Y.; Rhind-Tutt, A. J.; Sheft, I.; Vernon, C. A. *J. Chem. Soc.* **1961**, 3240.
(36) Wallace, J. E.; Schroeder, L. R. *J. Chem. Soc., Perkin Trans. 2* **1976**, 1632.

DOI: 10.1021/acs.joc.6b00860
J. Org. Chem. 2016, 81, 5949−5962

(37) Zhang, Z.; Ollmann, I. R.; Ye, X.-S.; Wischnat, R.; Baasov, T.; Wong, C.-H. *J. Am. Chem. Soc.* **1999**, *121*, 734.
(38) Li, X.; Huang, L.; Hu, X.; Huang, X. *Org. Biomol. Chem.* **2009**, *7*, 117.
(39) Blackmond, D. G. *Acc. Chem. Res.* **2000**, *33*, 402.
(40) Blackmond, D. G. *Tetrahedron: Asymmetry* **2010**, *21*, 1630.
(41) Blackmond, D. G. *J. Am. Chem. Soc.* **2015**, *137*, 10852.
(42) Nokami, T.; Shibuya, A.; Manabe, S.; Ito, Y.; Yoshida, J.-i. *Chem. - Eur. J.* **2009**, *15*, 2252.
(43) Garcia, B. A.; Gin, D. Y. *J. Am. Chem. Soc.* **2000**, *122*, 4269.
(44) Wever, W. J.; Cinelli, M. A.; Bowers, A. A. *Org. Lett.* **2013**, *15*, 30.
(45) Amatore, C.; Jutand, A.; Mallet, J.-M.; Meyer, G.; Sinay, P. *J. Chem. Soc., Chem. Commun.* **1990**, 718.
(46) Kremer, K. A. M.; Helquist, P. *J. Organomet. Chem.* **1985**, *285*, 231.
(47) Juaristi, E.; Cuevas, G. *Tetrahedron* **1992**, *48*, 5019.
(48) Boons, G.-J.; Stauch, T. *Synlett* **1996**, *1996*, 906.
(49) Pilgrim, W.; Murphy, P. V. *J. Org. Chem.* **2010**, *75*, 6747.
(50) Cumpstey, I. *Org. Biomol. Chem.* **2012**, *10*, 2503.
(51) Rencurosi, A.; Lay, L.; Russo, G.; Caneva, E.; Poletti, L. *J. Org. Chem.* **2005**, *70*, 7765.
(52) Rencurosi, A.; Lay, L.; Russo, G.; Caneva, E.; Poletti, L. *Carbohydr. Res.* **2006**, *341*, 903.
(53) Fernandez, E. J.; Laguna, A.; Lopez-de-Luzuriaga, J. M.; Monge, M.; Nema, M.; Olmos, M. E.; Perez, J.; Silvestru, C. *Chem. Commun.* **2007**, 571.
(54) Soran, A. P.; Silvestru, C.; Breunig, H. J.; Balázs, G.; Green, J. C. *Organometallics* **2007**, *26*, 1196.
(55) Haiges, R.; Rahm, M.; Dixon, D. A.; Garner, E. B.; Christe, K. O. *Inorg. Chem.* **2012**, *51*, 1127.
(56) Pandey, K. K.; Patidar, P.; Tiwari, P. *Polyhedron* **2012**, *34*, 84.
(57) Reith, L. M.; Stiftinger, M.; Monkowius, U.; Knör, G.; Schoefberger, W. *Inorg. Chem.* **2011**, *50*, 6788.
(58) Moilanen, J.; Ganesamoorthy, C.; Balakrishna, M. S.; Tuononen, H. M. *Inorg. Chem.* **2009**, *48*, 6740.
(59) Bauza, A.; Quinonero, D.; Deya, P. M.; Frontera, A. *Phys. Chem. Chem. Phys.* **2012**, *14*, 14061.
(60) Monakhov, K. Y.; Linti, G. *Inorg. Chem.* **2009**, *48*, 6986.
(61) Auer, A. A.; Mansfeld, D.; Nolde, C.; Schneider, W.; Schürmann, M.; Mehring, M. *Organometallics* **2009**, *28*, 5405.
(62) Jang, Y. H.; Goddard, W. A. *J. Phys. Chem. B* **2002**, *106*, 5997.
(63) Pudar, S.; Oxgaard, J.; Chenoweth, K.; van Duin, A. C. T.; Goddard, W. A. *J. Phys. Chem. C* **2007**, *111*, 16405.
(64) Becke, A. D. *Phys. Rev. A: At., Mol., Opt. Phys.* **1988**, *38*, 3098.
(65) Vosko, S. H.; Wilk, L.; Nusair, M. *Can. J. Phys.* **1980**, *58*, 1200.
(66) Lee, C. T.; Yang, W. T.; Parr, R. G. *Phys. Rev. B: Condens. Matter Mater. Phys.* **1988**, *37*, 785.
(67) Stephens, P. J.; Devlin, F. J.; Chabalowski, C. F.; Frisch, M. J. *J. Phys. Chem.* **1994**, *98*, 11623.
(68) Grimme, S.; Antony, J.; Ehrlich, S.; Krieg, H. *J. Chem. Phys.* **2010**, *132*, 154104.
(69) Goerigk, L.; Grimme, S. *Phys. Chem. Chem. Phys.* **2011**, *13*, 6670.
(70) Martin, A.; Arda, A.; Désiré, J.; Martin Mingot, A.; Probst, N.; Sinaÿ, P.; Jiménez Barbero, J.; Thibaudeau, S.; Blériot, Y. *Nat. Chem.* **2016**, *8*, 186.
(71) Nokami, T. *Trends Glycosci. Glycotechnol.* **2012**, *24*, 203.
(72) Nokami, T.; Nozaki, Y.; Saigusa, Y.; Shibuya, A.; Manabe, S.; Ito, Y.; Yoshida, J.-i. *Org. Lett.* **2011**, *13*, 1544.
(73) Zeng, Y.; Wang, Z.; Whitfield, D.; Huang, X. *J. Org. Chem.* **2008**, *73*, 7952.
(74) Crich, D.; Dai, Z.; Gastaldi, S. *J. Org. Chem.* **1999**, *64*, 5224.
(75) Paulsen, H.; Herold, C.-P. *Chem. Ber.* **1970**, *103*, 2450.
(76) Pedersen, C. M.; Nordstrøm, L. U.; Bols, M. *J. Am. Chem. Soc.* **2007**, *129*, 9222.
(77) Trumtel, M.; Tavecchia, P.; Veyrières, A.; Sinaÿ, P. *Carbohydr. Res.* **1989**, *191*, 29.

DOI: 10.1021/acs.joc.6b00860
J. Org. Chem. 2016, 81, 5949−5962